

Multiplexed, quantitative serological profiling of COVID-19 from a drop of blood by a point-of-care test

Authors: Jacob T. Heggstad^{1†}, David S. Kinnamon^{1†}, Lyra B. Olson², Jason Liu¹, Garrett Kelly¹, Simone A. Wall¹, Cassio M. Fontes¹, Daniel Y. Joh^{1,3}, Angus M. Hucknall¹, Carl Pieper⁴, Ibtehaj A. Naqvi⁵, Lingye Chen⁶, Loretta G. Que⁶, Thomas Oguin III⁷, Smita K. Nair^{5,8}, Bruce A. Sullenger^{1,5,9}, Christopher W. Woods^{7,10}, Gregory D. Sempowski⁷, Bryan D. Kraft⁶, Ashutosh Chilkoti¹

Affiliations:

¹ Department of Biomedical Engineering, Pratt School of Engineering, Duke University, Durham, NC 27708 USA

² Duke Medical Scientist Training Program, Department of Pharmacology and Cancer Biology, Duke University School of Medicine, Durham, NC 27710 USA

³ Division of Plastic, Maxillofacial, and Oral Surgery, Department of Surgery, Duke University Medical Center, Durham NC 27710 USA

⁴ Departments of Biostatistics and Bioinformatics, Duke University Medical Center, Durham, NC 27708 USA

⁵ Department of Surgery, Duke University School of Medicine, Durham, NC 27710 USA

⁶ Division of Pulmonary, Allergy, and Critical Care Medicine, Department of Medicine, Duke University Medical Center, Durham, NC 27710 USA

⁷ Department of Medicine and Duke Human Vaccine Institute, School of Medicine, Duke University, Durham, NC 27710 USA

⁸ Department of Neurosurgery and Pathology, Duke University School of Medicine, Duke University, Durham, NC 27710 USA

⁹ Department of Pharmacology and Cancer Biology, Duke University School of Medicine, Durham, NC 27710 USA

¹⁰ Center for Applied Genomics and Precision Medicine, Department of Medicine, Duke University, Durham, NC 27710 USA

[†]These authors contributed equally to this work.

Abstract

Highly sensitive, specific, and point-of-care (POC) serological assays are an essential tool to manage the COVID-19 pandemic. Here, we report on a microfluidic, multiplexed POC test that can profile the antibody response against multiple SARS-CoV-2 antigens—Spike S1 (S1), Nucleocapsid (N), and the receptor binding domain (RBD)—simultaneously from a 60 μ L drop of blood, plasma, or serum. We assessed the levels of anti-SARS-CoV-2 antibodies in plasma samples from 19 individuals (at multiple time points) with COVID-19 that required admission to the intensive care unit and from 10 healthy individuals. This POC assay shows good concordance with a live virus microneutralization assay, achieved high sensitivity (100%) and specificity (100%), and successfully tracked the longitudinal evolution of the antibody response in infected individuals. We also demonstrated that we can detect a chemokine, IP-10, on the same chip, which may provide prognostic insight into patient outcomes. Because our test requires minimal user intervention and is read by a handheld detector, it can be globally deployed in the fight against COVID-19 by democratizing access to laboratory quality tests.

40 Introduction

41 The ongoing severe acute respiratory syndrome–coronavirus 2 (SARS-CoV-2) pandemic poses an
42 enormous challenge to the world. SARS-CoV-2 has resulted in over 47 million cases of coronavirus disease
43 (COVID-19) worldwide, resulting in over 1.2 million deaths as of November 3, 2020¹. Unlike many other viruses,
44 SARS-CoV-2 displays high infectivity, a large proportion of asymptomatic carriers, and a long incubation time of
45 up to 12 days, during which carriers are infectious²⁻⁴. As a result, transmission has been widespread, resulting
46 in overwhelmed healthcare capacities across the globe^{5,6}. Timely, reliable and accurate diagnostic and
47 surveillance tests are necessary to control the current outbreak and to prevent future spikes in transmission.

48 Reverse transcription polymerase chain reaction (RT-PCR), which detects viral nucleic acids, is the current
49 gold standard for COVID-19 diagnosis^{7,8}. Although RT-PCR is highly sensitive and specific^{9,10}, it does not detect
50 past infections—RNA is typically only present at high quantities during acute infection—and it does not provide
51 insight into the host’s response to infection¹¹. Serological assays, which detect antibodies induced by SARS-
52 CoV-2, are a crucial supplement to nucleic acid testing for COVID-19 management^{12,13}. Specifically, serological
53 assays are important to track the body’s immune response¹⁴, and to potentially inform prognosis¹⁵ or immunity
54 status¹². Serological assays are also essential for use in epidemiological studies¹⁶, and are a critical enabling
55 tool for vaccine development¹⁷.

56 SARS-CoV-2 is an enveloped RNA virus with four structural proteins: spike (S) protein, membrane (M)
57 protein, enveloped (E) protein, and nucleocapsid (N) protein¹⁸. As the pandemic unfolded, several serological
58 binding assays were developed including enzyme-linked immunosorbent assays (ELISAs) and lateral flow
59 assays (LFA). These assays measure either the level of total antibody or that of specific antibody isotypes that
60 bind to viral proteins—normally S or N. Several studies have demonstrated promising clinical sensitivity and
61 specificity for ELISA and some LFAs^{19,20}. Furthermore, several ELISAs have been shown to correlate well with
62 neutralizing antibody titers^{21,22}, and thus may be useful clinically and in vaccine development²³. However, both
63 ELISA and LFAs have major disadvantages that limit their applicability for COVID-19 management. ELISA
64 requires technical expertise, laboratory infrastructure, and multiple incubation and wash steps, limiting its
65 applicability to settings outside of a centralized laboratory²⁴. On the other hand, LFAs are portable, but they
66 have lower sensitivity and provide qualitative results²⁵, whereas a quantitative readout is preferred for clinical
67 use, research studies, and surveillance applications. Collectively, these shortcomings of ELISAs and LFAs
68 motivate the need for an easily deployable, point-of-care test (POCT) that can be manufactured in large volumes,
69 has quantitative figures of merit equal to laboratory-based tests, and is as easy to use as an LFA.

70 To address the challenge of creating a user-friendly and widely deployable assay that can detect prior
71 exposure to, and immunological response against SARS-CoV-2, we developed a new multiplexed portable
72 COVID-19 serological assay that is described herein. Our passive microfluidic platform provides sensitive and
73 quantitative detection of antibodies against multiple SARS-CoV-2 viral antigens in 60 minutes with a single test
74 from a single 60 μ L drop of blood, plasma, or serum. We chose to quantify the antibody response against three
75 different SARS-CoV-2 antigens because emerging studies have demonstrated that the primary antigenic target
76 of the humoral immune response may inform disease progression and prognosis¹⁴. Thus, being able to
77 differentiate the viral targets of antibodies—as we can with our platform—may be especially valuable. Further,
78 our portable test is completely automated and can function independently of a centralized laboratory at the point-
79 of-care. We also show that our test can be easily modified to detect additional protein biomarkers, such as
80 cytokines/chemokines, without compromising the performance of the serological assay, which may provide
81 further clinical insight into disease severity and or patient outcomes^{2,26,27}. Collectively, these attributes suggest
82 that our platform is a valuable tool for COVID-19 management both at the individual patient level (i.e. monitoring
83 patients who may progress to severe disease) and for large-scale epidemiological studies at the population level.

84 Results

85 The DA-D4 point-of-care test (POCT) for 86 COVID-19 serology

87 Our strategy to evaluate the
88 antibody response to SARS-CoV-2 is
89 based on the D4 assay platform,
90 developed recently and reported
91 elsewhere²⁸. The D4 platform is a
92 completely self-contained immunoassay
93 platform fabricated upon a “non-fouling”
94 poly(oligoethylene glycol methyl ether
95 methacrylate) (POEGMA) brush, where
96 all reagents needed to complete the
97 assay are inkjet printed directly onto the
98 surface. In previous work, we have used
99 this platform for the detection of several
100 protein biomarkers using a fluorescent
101 sandwich immunoassay format²⁸. Here,
102 we modified the design of the assay to
103 detect antibodies against SARS-CoV-2
104 using a double-antigen (DA) bridging
105 immunoassay format, which detects total
106 antibody (all isotypes and subclasses).
107 The DA-D4 is fabricated by inkjet printing
108 viral antigens as stable and spatially
109 discrete capture spots. In addition, viral
110 antigens are labeled with a fluorescent
111 tag and are printed nearby on an
112 excipient pad as dissolvable spots.
113 When a sample is added to the assay
114 (**Fig. 1a-i**), the excipient pad dissolves
115 and liberates the fluorescently labeled
116 antigen (**Fig. 1a-ii**), which then diffuses
117 across the polymer brush to the capture
118 spots and labels any antibody that has
119 been captured from solution by the
120 stable capture spots of unlabeled
121 antigen (**Fig. 1a-iii**). The fluorescence
122 intensity of the capture spots is then
123 imaged using a fluorescent detector and
124 scales with antibody concentration in a
125 sample (**Fig. 1a-iv**). Because capture
126 spots of each antigen are printed at
127 spatially discrete locations, this design
128 enables multiplexed quantification of
129 multiple target antibodies using a single

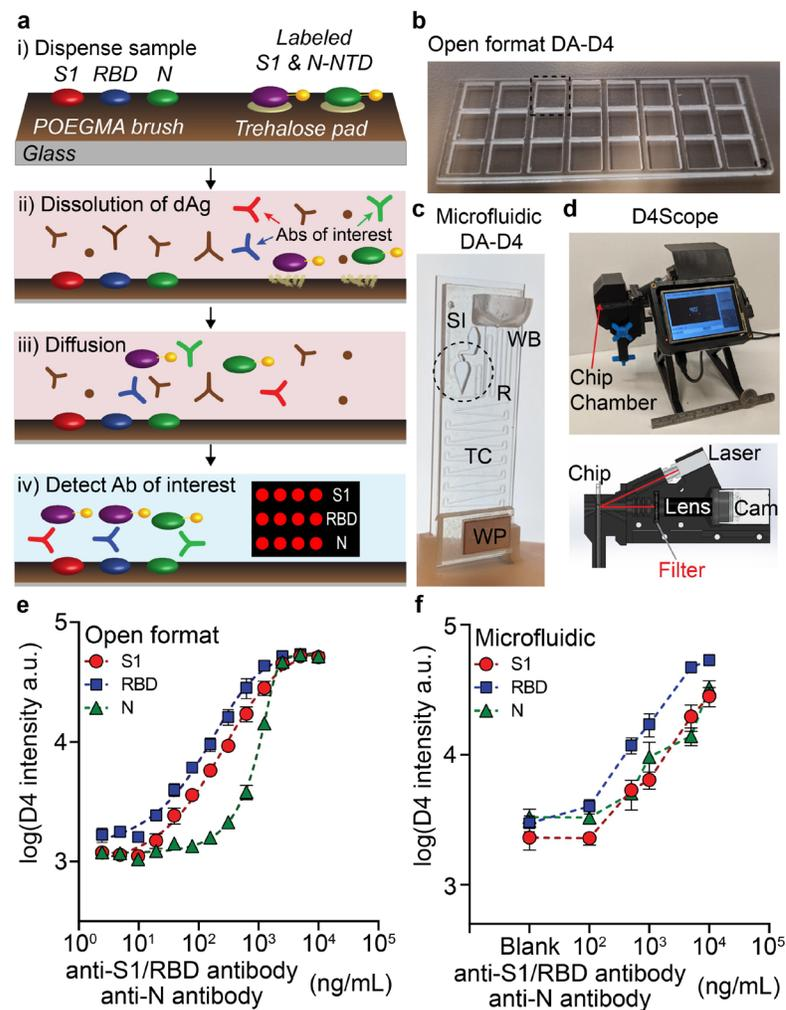


Figure 1. DA-D4 POCT schematic and analytical validation. (a) DA-D4 assay chip schematic. S1, RBD, and N capture antigens and fluorescently labeled S1 and N-NTD detection antigens (dAg) are inkjet printed onto a POEGMA substrate. When a sample is added, dAg are liberated from the surface due to the dissolution of the underlying trehalose pad. Antibodies targeting each viral antigen then bridge the capture antigens to the dAg, resulting in a fluorescence signal that scales with antibody concentration. **(b)** Open format DA-D4 with 24-individual assays. **(c)** Microfluidic DA-D4. Sample is added to the sample inlet (SI), filling the reaction chamber (RC) which contains the assay reagents. Wash buffer is added to the wash buffer reservoir (WB) which chases the sample through the microfluidic cassette. The timing channel (TC) sets the incubation time. All liquid is eventually soaked up by the wicking pad (WP) after the incubation process. The size is that of a standard microscope slide. **(d)** D4Scope and cut-away view of the optical path. The microfluidic flow cell is inserted on the left, and pressing a button automates laser excitation, camera exposure, and data output. **(e)** Analytical validation of the open format DA-D4. Antibodies targeting each antigen were spiked into undiluted human serum and incubated for 30 min. Each data point represents the average of three independent runs, and the errors bars represent the standard error of mean (SEM). **(f)** Analytical validation of microfluidic DA-D4. Each data point for an antigen represents the average of four independent microfluidic flow cells and error bars represent the SEM.

130 fluorescent tag, which greatly simplifies the detector design and assay readout.

131 To fabricate a serological assay for SARS-CoV-2, nucleocapsid (N), spike S1 domain (S1), and the
132 receptor-binding domain (RBD) of S1 were inkjet printed as the “stable” capture reagents onto POEGMA-coated
133 slides. Our rationale for simultaneously assaying the antibody response towards N, S1, and RBD antigens is that
134 it is not fully understood which epitopes elicit an immune response in all individuals, though they are all believed
135 to be immunogenic^{29,30} and because studies have shown that the primary target of the immune response may
136 inform disease prognosis¹⁴. N is expressed abundantly by SARS-CoV-2 during infection and is highly
137 immunogenic in other coronaviruses^{31,32}. The S protein—composed of the S1 and S2 domains—is exposed on
138 the viral coat of SARS-CoV-2 and plays an essential role in viral attachment, fusion, entry, and transmission³³.
139 Because S2 is highly conserved across many coronaviruses and is thus potentially cross-reactive, S1 was
140 chosen for antibody detection³⁴. RBD—the portion of S1 that binds cells expressing viral receptor—is the target
141 for many neutralizing antibodies and is thus a promising antigenic target for serological assays³⁴. **Fig. S1a**
142 shows the layout and dimensions of an open format DA-D4 chip. Each chip contains 24 individual assays with
143 S1, RBD, and N antigens arrayed as separate rows of five identical ~170 µm diameter spots. Next, fluorescent
144 conjugates of S1—which contains the amino acid sequence for RBD—and the N-terminal domain (NTD) of N
145 (produced in-house, see **Fig. S2** for SDS-PAGE of expression and purification) were mixed 1:1 and inkjet printed
146 as twelve identical 1 mm diameter spots on an identically sized trehalose pad (**Fig S1a**). N-NTD —instead of
147 full-length N— was chosen as the detection reagent because the full N domain can dimerize in solution,
148 potentially leading to a false positive result in the DA format³⁵.

149 Analytical validation of the DA-D4 POCT using simulated samples

150 We first sought to demonstrate that the DA-D4 assay can detect antibodies against recombinantly
151 expressed SARS-CoV-2 antigens. Initially, the analytical performance was characterized using the open format
152 DA-D4 (**Fig. 1b**). This is because the open format DA-D4 assay has been extensively optimized and
153 characterized by our group and has extremely high analytical sensitivity which enables us to determine the
154 figures-of-merit that are theoretically possible for a particular D4 assay. A disadvantage of the open format DA-
155 D4 assay, however, is that it requires a rinse step by the user after incubation of the sample²⁸.

156 For point-of-care deployment and an improved user experience, we developed—in the course of this
157 study—a new, gravity and capillary driven “passive” microfluidic flow cell that fully automates the assay (**Fig.**
158 **1c**). The microfluidic flow cell is fabricated by adhering complementary layers of precision laser-cut acrylic and
159 adhesive sheets onto the functionalized POEGMA substrate (**Fig. S3** and **Fig. S1b** for the print layout). The
160 resulting microfluidic flow cell features a reaction chamber, timing channel, sample inlet, wash buffer reservoir,
161 and wicking pad that automates the sample incubation, sample removal, wash, and drying steps. This simplifies
162 the user experience and limits the possibility of a user incorrectly carrying out the test, as it only requires the
163 user to add the sample and a drop of wash buffer to the cassette. After ~60 minutes, the cassette is ready for
164 imaging with a custom-built fluorescent detector—the D4Scope (**Fig. 1d**).

165 The D4Scope is a low-cost (<\$1,000), portable fluorescence detector (with dimensions of 7 inches wide,
166 6 inches tall, 5 inches deep and a weight of ~5 pounds; see **Fig. S4** for dimensions and image) built from off-
167 the-shelf components and assembled using 3D-printed parts that can image microarray spots with high
168 sensitivity. It utilizes coherent 638 nm red laser light set at an oblique angle (30°) relative to the surface to excite
169 the fluorescently labeled antigens. The fluorescence wavelength emission from the labeled reagents is then sent
170 through a bandpass filter and imaged with a high-efficiency Sony IMX CMOS sensor in a Basler Ace camera
171 (**Fig. 1d**). This setup provides a large field-of-view of 7.4 mm x 5 mm and a fine (raw) lateral resolution of ~2.4
172 µm. A user-friendly interface was developed in Python that runs on a 3.5” Raspberry Pi touchscreen to control
173 laser excitation, camera exposure, and image file output (see supplementary information for more details, **Fig.**
174 **S4**).

175 To mimic seropositive samples, we spiked commercially available antibodies (with known binding affinity
176 towards SARS-CoV-2 antigens) into undiluted pooled human serum that was collected prior to the COVID-19

177 outbreak. A dilution series spanning four logs was evaluated on open format DA-D4 chips and yielded a dose-
 178 response curve with fluorescence intensities that scaled with antibody concentration and approximated a
 179 sigmoidal curve, demonstrating that the assay was responsive to the antibodies of interest (**Fig. 1e**). Within the
 180 microfluidic flow cell, the chamber geometry, reagent spacing/alignment, and amount of printed reagent were
 181 iteratively optimized to match the performance metrics of the open format DA-D4. Six doses (including a blank)
 182 with varying amounts of anti-S1/RBD and anti-N antibodies were prepared and tested in quadruplicate on 24
 183 separate microfluidic flow cells to demonstrate equivalence between the open format (**Fig.1b**) and microfluidic
 184 flow cell (**Fig.1c**). In the microfluidic flow cell, the fluorescence intensity of the capture antigens—imaged with
 185 the D4Scope—also scaled with antibody concentration, suggesting that the test is responsive to anti-SARS-
 186 CoV-2 antibodies (**Fig. 1f**).

187 Clinical validation of the DA-D4 POCT

188 Next, we sought to validate the clinical performance of the DA-D4 POCT in a
 189 retrospective study using banked plasma samples from patients with PCR-confirmed
 190 COVID-19 who had been admitted to the intensive care unit (ICU) at Duke University
 191 Medical Center. A total of 34 COVID-19 positive plasma samples (heat-inactivated)
 192 from 19 patients—some of which had longitudinal samples available—and 10
 193 negative samples (collected prior to the COVID-19 pandemic) were tested on the
 194 microfluidic DA-D4 and imaged with the D4Scope. The median age of the COVID-19
 195 patients was 55. Of the 19 patients, 10 were female and 9 were male. For most patients,
 196 the date of symptom onset was known (29 out of 34 samples), where the average was
 197 20.7 days with a range of 6–48 days. The complete patient profile is provided in **Table**
 198 **S1**.
 199
 200
 201
 202
 203
 204
 205
 206
 207
 208

209 Antibody reactivity towards all three viral antigens was measured on single
 210 microfluidic flow cell for each patient sample. For validation, we conservatively assigned
 211 the threshold for a positive test result as three standard deviations above the mean of the
 212 negative controls. There was a statistically significant difference between the mean
 213 intensity for COVID-19 positive and negative samples ($p < 0.0001$) for all three markers
 214 (**Fig. 2a-c**). 33 out of 34 (97.1%) COVID-19 positive samples tested above the threshold
 215 for anti-S1 and anti-N, while 34 out of 34 (100%) tested positive for anti-RBD. All
 216 negative controls tested below the threshold
 217
 218
 219
 220
 221
 222
 223

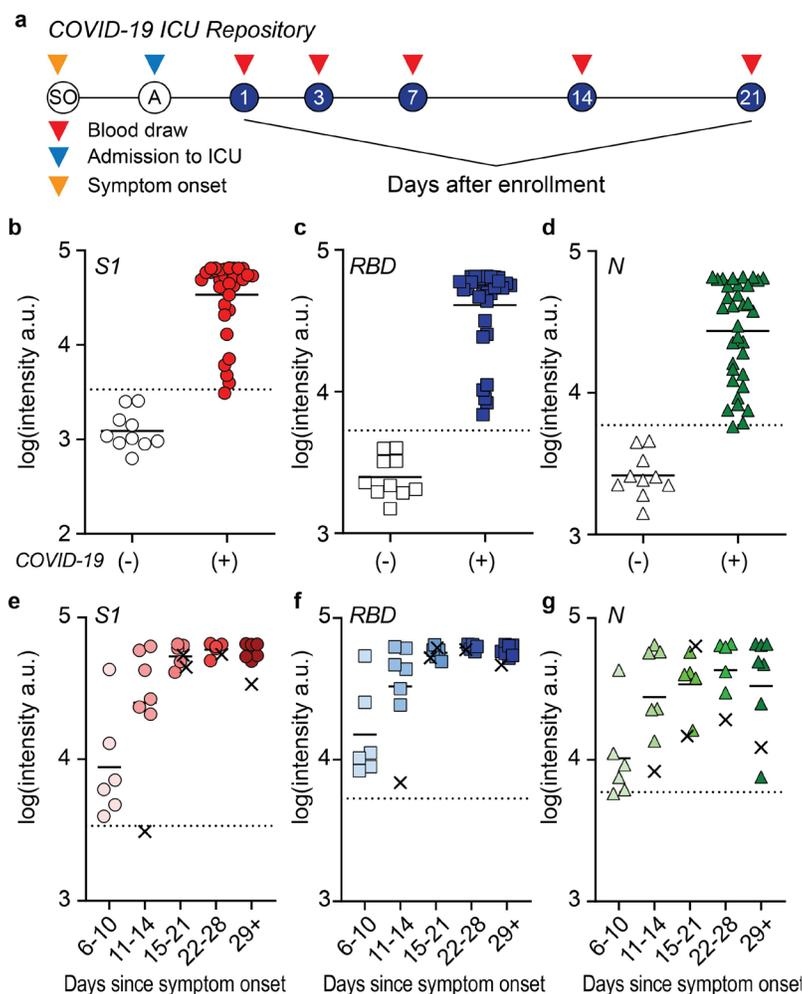


Figure 2. Clinical validation study. (a) Study design for COVID-19 ICU Biorepository samples. Patients at Duke University Medical Center were enrolled into the study after admission to the ICU. Blood draws were taken at days 1, 3, 7, 14 and 21 after enrollment until discharge or death occurred. (b-d) Aggregated data for 34 positive samples and 10 negative controls tested for antibodies against (b) S1, (c) RBD, and (d) N. Dashed lines represent 3 standard deviations above the mean of the negative controls and solid line represents the mean of each group. (e-g) Data from b-d partitioned by days since symptom onset. For 5 samples, date since symptom onset was unknown so days since first positive COVID-19 test was used (marked with an x).

for each marker (specificity of 100%). Representative images for a high positive and negative sample are included in **Figure S5**.

Next, we partitioned the data into five different groups based on days since symptom onset: 6–10 days, 11–14 days, 15–21 days, 22–28 days, and > 29 days (**Fig. 2d-f**). For two patients (five total samples), the date of symptom onset was unknown, hence the day since first positive PCR test result was used instead (these data points are marked with an x). When the data are partitioned by date since symptom onset, the sensitivity for all three markers included in our test increased to 100% for 15 days or longer after symptom onset. For antibodies targeting S1 and RBD, we found a statistically significant difference between the different time groups, as determined by one-way ANOVA ($p < 0.0001$). Multiple comparisons by Tukey's post hoc testing revealed that the magnitude of the antibody response to S1 and RBD was higher in all groups after 11 days compared to days 6–10 ($p < 0.05$) and that there was no statistically significant ($p > 0.05$) difference between any group after day 11. These results suggest that our assay spans a useful temporal range to detect the dynamic production of antibodies that typically occurs within 2 weeks of symptom onset¹⁵. In addition, the patients tested all developed a robust and sustained antibody response against S1 and RBD.

For antibodies targeting N, there was also a statistically significant difference in DA-D4 readout between groups as determined by one-way ANOVA ($p < 0.05$). However, the production of N-targeting antibodies appears to occur later, as there was no statistically significant difference in the antibody response when comparing days

6 – 10 and 11 – 14 ($p > 0.05$), but all groups after 15 days were significantly higher than the first time point ($p < 0.05$). The concentration of N-targeting antibodies also appears to be more variable across all patients, especially at later time points, with some samples testing close to the threshold value. This could be due to the fact that some patients may develop a stronger response against other viral antigens/epitopes (RBD or S1)³⁶ or against an epitope of N not within the NTD, highlighting the importance of testing for antibodies against several antigens simultaneously to maximize test sensitivity and specificity.

We also conducted a proof-of-concept study using whole human blood as the sample source for the microfluidic flow cell, to demonstrate that the DA-D4 assay can be used at the point-of-care or the point-of-sample collection without the need for any sample processing. To do so, we made minor modifications (see section 7 of supplementary information, **Fig. S6**) to the microfluidic timing channel and reaction chamber to account for the non-Newtonian fluid mechanics of whole blood (**Fig. 3a**). Briefly, a gradual slope was added to the reaction chamber to prevent accumulation of red blood cells during washing, and the incubation channel was shortened to account for a reduced flow rate.

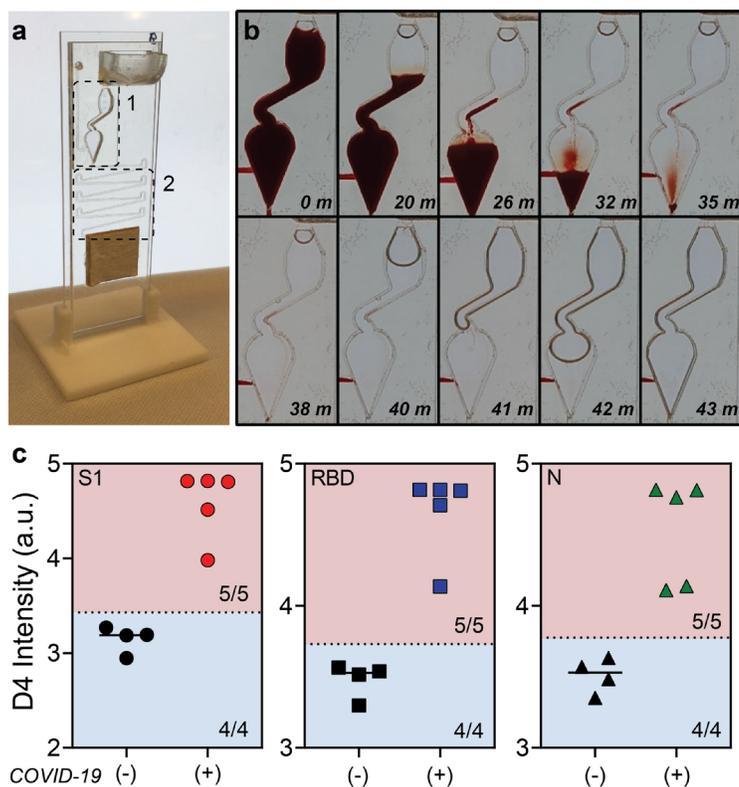


Figure 3. Testing whole blood. (a) Modified microfluidic flow cell for testing whole blood. Zone 1: the reaction chamber was modified to prevent red blood cells from collecting in the chamber. Zone 2: The incubation timing channel was shortened to compensate for the slower flow rate of blood and to ensure blood did not clot or clog the channels. (b) Time lapse of blood and wash buffer in the reaction chamber. (c) Aggregated data for 5 positive samples and 4 negative controls tested for antibodies against S1, RBD, and N. Dashed lines represent 3 standard deviations above the mean of the negative controls. 100% sensitivity (5/5) and 100% specificity (4/4) were achieved for S1, RBD, and N.

271 Fresh blood was collected in EDTA-coated tubes from four patients with negative COVID-19 antibody status (as
 272 as determined by ELISA performed by the supplier) and from five patients with confirmed COVID-19 (from new
 273 enrollments to the ICU study) (**Table S2**). Each 60 μ L blood sample was tested on the microfluidic DA-D4 assay.
 274 No complications were observed, such as coagulation of blood that can occur when testing whole blood in
 275 microfluidic systems. **Fig. 3b** shows representative images of the reaction chamber, with the time since sample
 276 addition noted in the lower right-hand corner of each sub-panel, demonstrating the ability of the microfluidic chip
 277 to process whole blood. The antibody response towards S1, RBD, and N from whole blood is shown in **Fig. 3c**.
 278 We set the threshold to determine a positive test as three standard deviations above the mean of the negatives.
 279 All negative samples tested as negative, and all positives tested above the threshold. These preliminary results
 280 suggest that the microfluidic DA-D4 assay is capable of detecting anti-SARS-CoV-2 antibodies in whole blood,
 281 so that the assay can be carried out immediately at the point of sample collection without the need for transport
 282 to a centralized laboratory for sample processing into serum or plasma and subsequent testing.

283 Monitoring antibody levels longitudinally

284 Having demonstrated the high clinical sensitivity and specificity of the microfluidic DA-D4 assay for
 285 detection of antibodies against SARS-CoV-2 antigens, as well as the ability to detect changes in antibody levels
 286 with time, we next sought to track individual patients to track their seroconversion. To accomplish this, we tested
 287 longitudinal plasma samples from

288 six individual patients (**Fig. 4a-f**).
 289 Across all six patients, the antibody
 290 response was initially low for the first
 291 time point tested and then increased
 292 and plateaued at later time points,
 293 consistent with the antibody
 294 dynamics reported in other studies
 295 ^{15,37,38}. The DA-D4 readout for
 296 antibodies targeting S1 and RBD
 297 appeared to saturate by the second
 298 time point—typically 2-3 weeks post
 299 symptom onset—suggesting that
 300 each patient mounted a strong and
 301 robust immune response that was
 302 sustained over time. For N, the
 303 dynamics were slower in one patient
 304 (#1) and did not fully saturate in
 305 another (#3), providing insight into
 306 the primary target of the antibody
 307 response in those patients. In
 308 general, patients with severe
 309 COVID-19 often develop very high
 310 antibody titers ³⁷, which is reflected
 311 in this ICU patient sample set by
 312 saturated signals at later time
 313 points. However, we were still able
 314 to measure seroconversion and
 315 antibody kinetics in each patient,
 316 suggesting that the DA-D4 is a
 317 useful tool for monitoring the

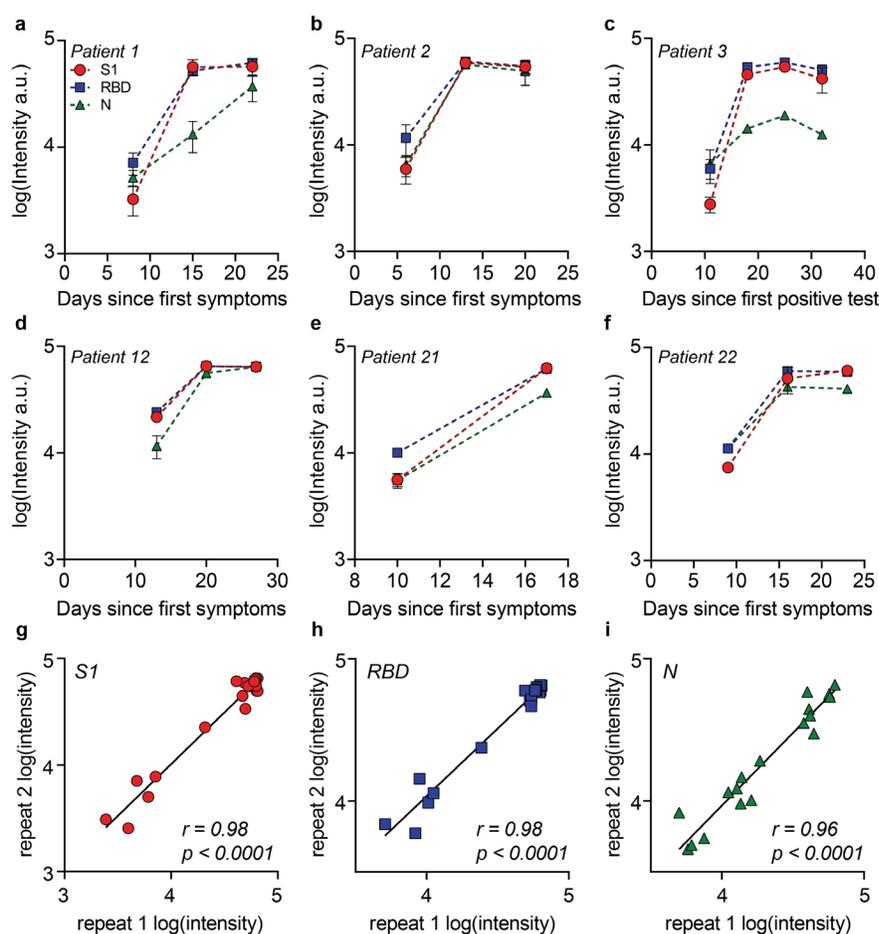


Figure 4. Longitudinal antibody tracking. (a-f) Six patients were tracked across multiple time points for antibodies targeting S1, RBD, and N. For patient 3 (c), date since symptom onset was unknown so days since first positive test was used. Each data point represents the average of two independent chips (with SD) run by separate users. (g-i) Data from parts a-f for each repeat. There is a strong correlation between each repeat for (g) S1, (h) RBD, and (i) N, with a Pearson r of 0.98, 0.98 and 0.96, respectively ($p < 0.0001$).

immune response. The earliest time points for each patient were also still elevated relative to the negative controls, indicating that we may have been able to detect seroconversion earlier, had samples from earlier time points been available. For patients later in disease progression with high antibody titers, dilutions could be performed to adjust the concentration into the linear range of the assay. Testing a sample at various dilutions would also allow us to calculate specific antibody titers, which we are not able to do from a single undiluted sample.

Each sample in the longitudinal study was tested in duplicate on different days and by a different user to characterize the reproducibility and robustness of our platform (**Fig. 4g-i**). We found a strong correlation for each marker, with a Pearson's r correlation of 0.98, 0.98, and 0.96 for S1, RBD, and N, respectively. The high correlation between replicates further emphasizes the quantitative nature and reproducibility of our platform for profiling the immune response to SARS-CoV-2.

Concordance with neutralizing antibody titers

We next compared the performance of the DA-D4 with a microneutralization assay that monitors functional neutralization of

SARS-CoV-2 via neutralizing antibodies binding to the RBD. All six patients that we tracked longitudinally developed robust neutralizing antibodies, and the microneutralization titer was strongly concordant with DA-D4 assay readout for antibodies targeting S1 and the RBD of S1 (**Fig. 5a-f**). Furthermore, a concordance analysis of the DA-D4 assay with the microneutralization assay for antibodies targeting S1 and RBD showed a strong correlation across all plasma samples tested (**Fig. S7a, b**), as determined by a Pearson $r > 0.70$ ($p < 0.0001$). For antibodies targeting N, the concordance between the two

assays was not as strong, with only a moderate correlation between the DA-D4 results and microneutralization data (**Fig. S7c**). This is expected, as N resides inside the capsid of SARS-CoV-2 and is not relevant for functional neutralization³⁹. This is also reflected in the longitudinal sample set. For example, patient #1 at day 15 after symptom onset has strong neutralizing antibodies, as seen by the microneutralization assay, despite a weak overall antibody level for N. Although future studies are required to validate the ability of neutralizing antibodies to confer protection, these results suggest that the DA-D4 assay could be used as a supplement to live virus neutralization assays, which typically require >48 hours and biosafety level 3 containment.

assays, which typically require >48 hours and biosafety level 3 containment.

Profiling prognostic biomarkers concurrent with serological testing

Finally, we investigated the feasibility of detecting a prognostic protein biomarker concurrent with serological profiling. This is motivated by the fact that others have identified potentially prognostic biomarkers that correlate well with disease severity and patient outcomes^{40,41}. Therefore, tracking antibody levels alongside

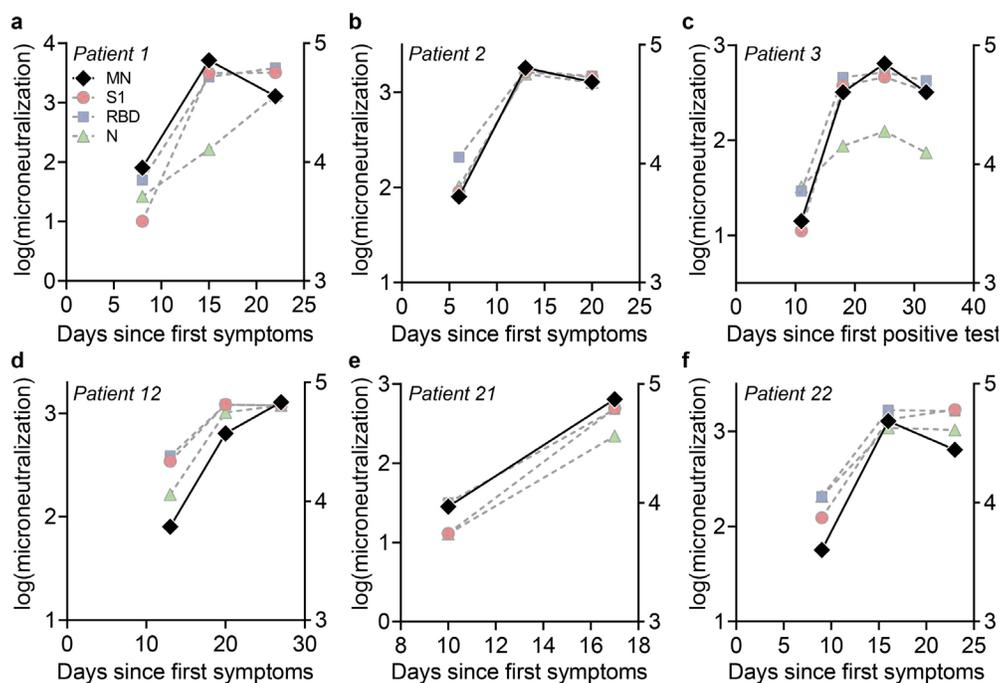


Figure 5. Correlation to microneutralization assay. (a-f) Microneutralization assays were performed on each longitudinal sample (black diamonds). Microneutralization titer is plotted on the left axis superimposed against the antibody data from figure 3 (plotted on the right axis).

365 prognostic biomarkers may provide clinically relevant information to inform interventions in the ICU for patients
 366 with a high probability of a poor outcome. As proof-of-concept, detection of IFN- γ -induced protein 10 (IP-10,
 367 CXCL10)—a chemokine that recruits inflammatory cells to the site of inflammation and which has been shown
 368 to be elevated in severe disease and correlates with patient prognosis^{27,41}—was integrated into the DA-D4 assay
 369 using a traditional sandwich immunoassay approach, as described previously²⁸.

370 Prior to testing patient samples, we sought to confirm that the multiplexed serological assay is compatible
 371 (not cross-reactive) with the IP-10 sandwich assay. To do so, we fabricated open format chips containing all
 372 necessary reagents for both COVID-19 serology and human IP-10 detection. First, we prepared a 15-point
 373 dilution series of recombinant human IP-10 spiked into fetal bovine serum (FBS)—spanning the relevant
 374 physiological range for COVID-19 patients identified elsewhere⁴¹—and added samples to chips in triplicate in
 375 the absence of antibodies targeting SARS-CoV-2 antigens. We observed a dose-dependent behavior for IP-10
 376 response with a low limit-of-detection of 0.12 ng/mL⁴² and minimal reactivity for
 377 SARS-CoV-2 capture antigens, confirming that the IP-10 assay components do not cross react with the
 378 serology components (**Fig. 6a**). Next, we prepared a dilution series of simulated
 379 seropositive samples and added them to the open format chips. Across all concentrations of anti-SARS-CoV-2
 380 antibodies, IP-10 capture antibody intensity was close to baseline, thus confirming that the serology components
 381 do not interfere with the IP-10 detection assay (**Fig. 6b**).

382 Having confirmed the compatibility of the IP-10 assay with multiplexed serology in the open D4
 383 format, we next sought to test the performance of our assay in patient samples. Ten COVID-19 positive plasma
 384 samples (from 7 patients) were procured from the ICU biorepository and were added undiluted to open format
 385 chips and then quantitatively assessed by the DA-D4. Separately, serum samples from the same patients were
 386 evaluated in parallel via LEGENDplex™ ELISA assay kits which report IP-10 concentration in pg/mL. We
 387 observed a strong positive correlation between the DA-D4 assay for IP-10 with ELISA across all 10 pairs of
 388 measurements, with a Pearson's r of 0.918 ($p = 0.0002$, 95% CI: 0.68 to 0.98) (**Fig. 6c**). We also tested
 389 for antibody reactivity towards S1, RBD, and N from the same samples and an additional sample of healthy
 390 pooled plasma (pre COVID-19 negative control) (**Fig. 6d**). Although we did not observe a strong relationship
 391 between antibody and IP-10 levels (data not shown),

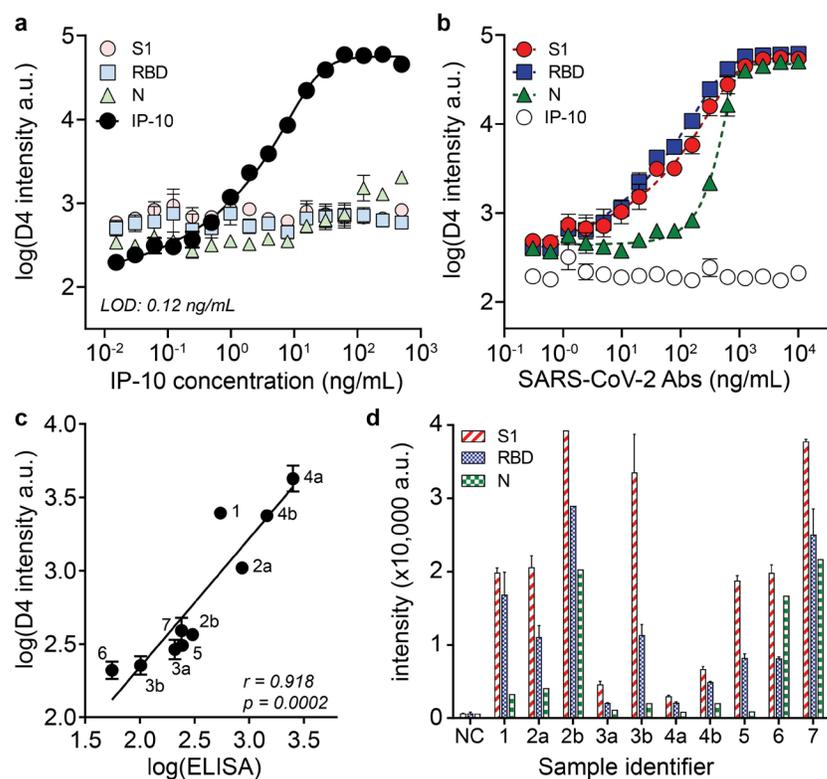


Figure 6. Combined prognostic biomarker and serology detection.

(a) Dose-response curve for recombinant IP-10 spiked into FBS. Each data point represents the average ($n = 3$) and error bars represent the SEM. The limit-of-detection (LOD) for IP-10 is 0.12 ng/mL. (b) Dose-response curve for anti-SARS-CoV-2 antibodies spiked into FBS. The highest concentration is 10 μ g/mL of anti-S1/RBD and 10 μ g/mL of anti-N antibodies. (c) Correlation between DA-D4 readout for IP-10 with an ELISA assay performed separately. Samples with a letter designate samples from one individual at different time points, where b occurs later in disease than a. All samples were tested in duplicate on the DA-D4 (with SD shown) except 2b (due to insufficient volume). (d) Antibody reactivity against S1, RBD, and N for sample tested in part c (with SD shown). NC = negative control pooled healthy plasma.

392 We also tested for antibody reactivity towards S1, RBD, and
 393 N from the same samples and an additional sample of healthy pooled plasma (pre COVID-19 negative control)
 394 (**Fig. 6d**). Although we did not observe a strong relationship between antibody and IP-10 levels (data not shown),

we did observe that in the patients for which we tested multiple samples, IP-10 decreased over time, while the levels of antibodies increased.

Overall, these results clearly show that the D4 assay format can simultaneously detect antibody response to foreign native SARS-CoV-2 antigens and a native protein biomarker from undiluted patient plasma. One of the benefits of detecting anti-SARS-CoV-2 antibodies from undiluted samples is that the sensitivity of the protein detection assay is not reduced because of dilution, allowing us to detect chemokines and cytokines—which are present at very low concentrations even during disease state—directly from complex biological milieu. Detection of additional prognostic biomarkers could also be implemented on the same chip, as long as there is no cross-reactivity between the assay reagents for serology and prognosis. Interestingly, a recent study found that the ratio of IL-6 to IL-10 can be used to guide clinical decision making⁴³, which we plan to measure in the next generation of this assay.

Discussion

As the COVID-19 pandemic unfolded, countries around the globe grappled with developing streamlined systems for diagnosis of acute infection using nucleic acid detection methods. Although there remains an urgent need for rapid and sensitive point-of-care tests for acute diagnosis, developing accurate and reliable serological assays has been deemed an equally important endeavor to complement existing diagnostic strategies^{12,44}. The challenge with developing an easy-to-use serology assay that can be broadly disseminated, but that performs as well as centralized laboratory-based methods is highlighted by the large number of ELISA and LFA tests that have been developed. While LFAs are portable and easy-to-use and ELISAs are quantitative and highly sensitive, there remains a need for a technology that can merge the best attributes of each format.

The DA-D4 POCT is a promising platform to supplement existing diagnostic technologies to manage the COVID-19 pandemic because it marries the best attributes of LFAs and ELISAs— it is quantitative, easy to use, widely deployable, requires only a single 60 μ L drop of blood, and can be performed with minimal user intervention. The SARS-CoV-2 DA-D4 assay can be used to measure antibody kinetics and seroconversion at the individual patient level directly from unprocessed blood or plasma. This test is highly sensitive and specific and is potentially suited for epidemiological surveillance at the population-level using low cost microfluidic cassettes that can be transported and stored for an extended period of time without a cold chain, and that require minimal user intervention to carry out the assay, which provide a quantitative readout using a low cost, hand-held detector.

We show a strong correlation between the DA-D4 assay readout (for S1 and the RBD of S1) and neutralizing antibody titers, suggesting that this test may be useful in understanding efficacy and durability of natural or vaccine-induced humoral immunity, and to potentially inform disease prognosis and population-level immunity. We also demonstrate that an additional prognostic biomarker can be easily incorporated into the test, which may be useful for monitoring disease severity and predict clinical outcomes. Combined, these attributes suggest this platform may also be useful on the individual patient level to aid in clinical decision making. While the results presented here mainly highlight the performance of the microfluidic chip, the open format architecture with up to 24 individual assays per glass slide may be useful for scenarios where higher throughput testing is demanded. The open format still has advantages compared to traditional ELISA because the open format only requires a single incubation step and one wash step, which reduces the hands-on time and equipment complexity required to complete the assay.

The DA-D4 has additional features that synergize to deliver a highly desirable serological assay. First, the double-antigen sandwich format (i.e. antibody bridging) has advantages over other serological assay formats. Because total antibody is detected rather than a single antibody isotype or subclass, seroconversion in patients can be detected earlier, which reduces the chances of a false negative result due to a test being administered too early in disease³⁸. Furthermore, because the labeled reagent does not have species specificity, the single assay kit could be used in pre-clinical vaccine development studies to measure antibody responses in

458 experimental animals²³. The lack of species-specific detection antibodies also reduces the risk of high
459 background signal caused by non-specific antibodies binding to the surface and subsequently being labeled⁴⁵.

460 Second, all reagents needed to complete the assay are incorporated onto the non-fouling PEOGMA
461 brush, which eliminates virtually all non-specific protein adsorption and cellular adhesion, thereby enabling an
462 extremely low LOD directly from undiluted samples⁴⁶⁻⁴⁸. Although many serological assays often dilute samples,
463 the ability to test undiluted samples is advantageous, especially when combined with prognostic biomarker
464 testing where dilution of low concentration analytes can lead to an undetectable signal. Testing multiple dilutions
465 can still be performed using our test when antibody levels become high, which could be used to calculate specific
466 titers. PEOGMA also acts as a stabilizing substrate for printed reagents, enabling long term storage of chips
467 without a cold chain²⁸. In this study, results were generated over the course of three months from the same
468 batch of tests stored in silica desiccated pouches at room temperature and ambient humidity.

469 Third, this platform can be easily multiplexed, which can be used to capture a more detailed picture of
470 the host immune response to SARS-CoV-2 infection by quantifying the antibody level induced to multiple viral
471 antigens—in this case N, S1, and S1-RBD—from a single sample without sacrificing ease-of-use. This is
472 because each viral antigen is deposited at a spatially discrete location, which allows for a single fluorescent tag
473 to be used during fluorescence imaging of the chip, thereby simplifying assay readout compared to other
474 multiplexing technologies such as Simoa or Luminex assays which rely on multiple different reporter molecules
475 and a more complex readout^{14,49}. This method also allows us to simultaneously measure the concentration of
476 potential prognostic biomarkers directly from plasma^{26,27} without compromising the performance of the
477 multiplexed serological assay. To the best of our knowledge, there are currently no tests on the market that can
478 probe for antibodies against multiple viral antigens and prognostic protein biomarkers simultaneously.

479 Fourth, this platform is designed for point-of-care deployment because it requires a single drop of blood
480 that is readily obtained from a fingerstick. This droplet is injected into the sample port of a gravity driven
481 microfluidic chip that requires no further user intervention beyond the concurrent addition of a few drops of wash
482 buffer into a separate port. The assay runs by itself under the action of gravity and capillary action until all the
483 fluid is drained from the microfluidic path by the absorbent pad at the bottom of the cassette, which fully absorbs
484 and contains all liquid. The microfluidic chip relies only upon capillary action and gravity to drive fluid flow, which
485 eliminates the need for pumps, valves, or actuators, and reduces the complexity and cost of the assay. This
486 enables the assay to be read out at the point of sample collection using the D4Scope—a highly sensitive and
487 inexpensive handheld detector developed to work with the microfluidic chip. The D4Scope images a chip and
488 provides a quantitative readout in less than 5 seconds, does not require an external power source or laboratory
489 infrastructure, and can wirelessly transmit the results to a remote server over Wi-Fi. While smartphone-based
490 diagnostics are becoming more popular, a benefit of this platform is that it does not rely on smartphone hardware
491 and software, which change rapidly. Combined, these attributes make our platform ideal for providing ELISA-like
492 sensitivity and quantitation with the ease-of-use and scalability of LFAs.

493 Where might this point of care assay for COVID-19 serology and prognosis be useful? Serial
494 quantification of antibody response and prognostic biomarkers would be most useful to monitor symptomatic and
495 severe cases where use of available therapeutics, such as antiviral or monoclonal therapies, is indicated.
496 Further, it could be used to screen for patients with poor antibody responses who may benefit from convalescent
497 plasma or monoclonal antibody therapy. We believe that this platform has potential utility in point-of-care settings
498 such as ICUs, urgent care clinics, and at the point-of-use—at locations where periodic surveillance of healthcare
499 workers and other essential workers in close proximity to others for extended periods of time such as assembly-
500 line manufacturing or food processing plants—is desirable to assist in tracking clusters of disease and
501 epidemiological studies. This platform could also be used as an inexpensive tool to study the longitudinal
502 dynamics of antibody levels to inform re-infection potential, as coronavirus immunity often lasts only ~6 months
503⁵⁰. Similarly, it could be used to monitor vaccine-induced humoral immunity, which could help determine if
504 boosters are needed in certain vaccinated individuals. This technology is suitable for low-resource settings

505 across the globe, where eliminating the need for sample storage and transport to a centralized testing facility,
506 and the attendant cold chain, is desirable, and where access to expensive, high-throughput clinical analyzers
507 that process large volumes of serology and other sandwich immunoassays is limited. Similarly, remote and
508 austere settings—such as the field-forward position of the military or other remote locations where pandemics
509 often emerge—can also benefit from this platform, as the testing is carried out with a disposable cassette and
510 a low-cost, light-weight, and handheld detector whose production can easily be scaled up to enable wide-spread
511 and dispersed deployment.

512 While the results presented here are promising, there are several issues identified during this study that
513 require further investigation prior to its deployment. First, our cohort of individuals with SARS-CoV-2 infection
514 consisted of adults with clinically significant disease, which is not representative of the entire spectrum of COVID-
515 19 disease severity. These samples were chosen to demonstrate proof-of-concept of the DA-D4 assay and
516 because these samples were locally available through an existing biobank. We recognize that a larger sample
517 size that spans the disease severity spectrum is required to develop a more robust measure of sensitivity and
518 specificity of the DA-D4 serology test for SARS-CoV-2. Similarly, we were not able to match demographics in
519 our negative control group, which may have introduced confounding variables in our analyses. Furthermore,
520 several of the samples we tested saturated the readout of our assay, which limits the dynamics we can measure
521 once high antibody titers are achieved. This limitation could be addressed by testing individual samples on
522 separate microfluidic chips at various dilutions, which would effectively increase the dynamic range of our assay
523 and yield more precise quantitative titer. Additionally, because of the double antigen design of our assay, we are
524 also not able to discriminate between specific antibody subclasses or isotypes, which has been shown to be
525 important for other diseases. Despite these limitations, we believe our assay is well poised to complement
526 existing diagnostic solutions once additional validation studies encompassing larger patient cohorts are
527 completed.

528 In summary, we have developed a COVID-19 serological assay that merges the benefits of LFAs and
529 ELISAs. We used this test to simultaneously measure the antibody levels for multiple viral antigens and a
530 potential prognostic biomarker directly from plasma and whole blood. For COVID-19 management, our platform
531 may be useful to better understand patient antibody responses, provide actionable intelligence to physicians to
532 guide interventions for hospitalized patients at the point-of-care, to assess vaccine efficacy, and to perform
533 epidemiological studies. Further, our platform is broadly applicable to other diseases where sensitive and
534 quantitative antibody and or protein detection is desirable in settings without access to a centralized laboratory.
535 Overall, we believe that our platform is a promising approach to democratize access to laboratory quality tests,
536 by enabling rapid and decentralized testing with minimal user intervention to locations outside the hospital.

537 **Materials and methods**

538 DA-D4 assay

539 The DA-D4 assay is based on the design of the D4 immunoassay, reported elsewhere²⁸. Briefly, a
540 polymer brush composed of poly(oligoethylene glycol methyl ether methacrylate) (POEGMA) was “grafted from”
541 a glass slide by surface-initiated atom transfer radical polymerization⁴⁷. Recombinant SARS-CoV-2 proteins
542 were then printed onto POEGMA-coated slides as capture and detection spots. Capture spots of the following
543 proteins were printed as ~170 μm diameter spots using a Scienion S11 sciFLEXARRAYER (Scienion AG) inkjet
544 printer: Spike S1 (Sino Biological, cat# 40591-V05H1), Spike RBD (Sino Biological, cat# 40592-V02H), and
545 Nucleocapsid protein (Leinco, cat# S854). Each protein was printed as a row/column of five identical spots. Next,
546 12 excipient pads of trehalose with 1.6 mm spacing were printed from a 10% (w/v) trehalose solution in deionized
547 water around the periphery of the capture antigen array using a BioDot AD1520 printer (BioDot, Inc.). To print
548 the detection reagents, S1 (Sino Biological, cat# 40591-V08H) and N-NTD (produced in-house), were first
549 conjugated to Alexa Fluor 647 (per the manufacturer’s instructions) and then detection spots, of the fluorescent
550 protein conjugates of these proteins were printed on top of the excipient pads as twelve 1 mm diameter spots.
551 A schematic of the chip that shows the spatial address and dimensions of the capture spots, trehalose pad and

detection spots is shown in **Figure S1**. After printing and final assembly, D4 chips were stored with desiccant until use. The amount of reagent deposited for the open-format and microfluidic format was identical, with the only difference being the relative spot placement (**Fig. S1a, b**). For DA-D4 assays that also detected IP-10, an additional column of five spots of capture antibody (R&D systems, cat# MAB266) was included and anti-IP-10 detection antibody (R&D systems, cat# AF-266) was included in the detection cocktail for the open format chips.

Fabrication and analytical testing of open format DA-D4

Open format slides were prepared by adhering acrylic wells to each slide, which splits one slide into 24 independent arrays (see **Fig. S1a** for a schematic and **Fig. 1b** for an image). To validate the analytical performance of the test, dose-response curves were generated using antibodies targeting SARS-CoV-2 antigens (Sino Biological, cat#: 40143-MM05, 40150-D001, and 40150-D004) spiked into undiluted pooled human serum. Open format chips were incubated with a 15-point dilution series (run in triplicate) for 30 minutes, briefly rinsed in a 0.1% Tween-20/PBS wash buffer and then dried. Arrays were imaged on an Axon Genepix 4400 tabletop scanner (Molecular Devices, LLC).

Fabrication and analytical testing of microfluidic DA-D4

The microfluidic chip fabrication process is described in detail in the supplementary information section 3. Briefly, the microfluidic chip was fabricated by adhering complementary layers of precision laser-cut acrylic and adhesive sheets onto the POEGMA substrate that had been functionalized with the relevant capture and detection reagents. The resulting assembly features a reaction chamber, timing channel, sample inlet, wash buffer reservoir, and wicking pad that automates the sample incubation, sample removal, wash, and drying steps. Simulated doses were prepared using antibodies targeting SARS-CoV-2 antigens (Sino Biological, cat#: 40143-MM05, 40150-D001, and 40150-D004) spiked into undiluted pooled human serum. Six doses (including a blank) were tested on the microfluidic DA-D4 in the following way: (1) The user dispenses 60 μ L of sample into the sample inlet using a pipette. (2) The user dispenses 135 μ L of wash buffer into the wash reservoir of the cassette using a pipette. (3) The user waits 60 minutes for the cassette to run to completion. During this time, (a) fluorescently labeled antigens dissolve and form sandwiches with the antibodies of interest and the immobilized capture antigen in the reaction chamber. (b) A small volume of sample traverses the timing channel, which governs the incubation time. (c) The sample reaches an absorbent pad situated at the end of the timing channel that rapidly wicks away all sample from the reaction chamber, ending incubation. (d) As the sample clears, wash buffer enters the reaction chamber removing residual sample and unbound reagent before it is also wicked away leaving a cleaned and dry imaging surface. We observed less than a \pm 10% variation in the designed 23-minute incubation time for the data presented in Figure 1f. The remaining difference in time accounts for washing and drying time. (4) The cassette is ready for analysis on the D4Scope. The vertical orientation of the cassette works in conjunction with the POEGMA brush to maintain low background fluorescence. Cellular and other sample debris can collect on the brush surface due to gravitational forces, even if no binding is occurring. The vertical orientation ensures that these debris fall harmlessly towards the timing channel during the wash step. This proved especially important when testing with undiluted human whole blood samples.

Clinical testing of microfluidic DA-D4

The same testing procedure as described in "*Analytical testing of microfluidic DA-D4*" was used to test both the plasma and whole blood clinical samples. For both cases, sample was added directly to the microfluidic DA-D4. For blood, a variation in the microfluidic design was used and is described in supplementary information section 7. This required the use of 200 μ L of wash buffer. All other procedures remained the same.

D4Scope fabrication and operation

The D4Scope design, fabrication, and assembly is described in detail in the supplementary information section 5. Briefly, the D4Scope's optical elements – the laser, bandpass filter, lens, and camera—and processing elements – the Raspberry Pi 4, touchscreen, and cabling—are mounted in a custom 3D printed chassis. Fully assembled, it weighs ~5 pounds. The D4Scope can be powered either through a portable battery pack or wall

598 power. Once connected to the power source, the D4Scope automatically runs our custom imaging Python
599 program. The user removes the light protection cover from the cassette loading port and slides the microfluidic
600 cassette with glass side towards the detector. The light protection cover is then replaced enclosing the cassette.
601 The user is then prompted to enter the sample ID # and chip ID # using either the touchscreen or optional
602 attached keyboard and mouse.

603 The D4Scope has two fine adjustment knobs on the cassette loading port that allow for precise vertically
604 and horizontally movement of the cassette relative to the laser source to ensure that the DA-D4 array is perfectly
605 centered with the excitation source. Each array has co-printed two control spots that will always be uniformly
606 bright across all tested samples and align with two super-imposed alignment cross hairs on the live video-feed
607 of the D4Scope. Using the “Toggle video” function on the UI activates the laser and camera to provide a live
608 view of the imaging area for this alignment. Once aligned, the “Toggle video” function can be pressed again to
609 end the live view, and the “Capture image” function can be used to collect and save the resulting image onto the
610 on-board hard-drive and optionally to a cloud-based server defined by the end-user. The live-view feature should
611 be used sparingly to prevent photo-bleaching of the sample. For this study we manually analyzed the resulting
612 fluorescence intensity using Genepix Analysis software. However, we have developed an algorithm for automatic
613 analysis of spot intensity and instantaneous results on our open-format platform, which will be reported
614 elsewhere.

615 Patient samples

616 De-identified heat-inactivated EDTA plasma samples (57°C for 30 minutes) were accessed from the Duke
617 COVID-19 ICU biorepository (Pro00101196, PI Bryan Kraft) via an exempted protocol approved by the Duke
618 University Institutional review board (Pro00105331, PI Ashutosh Chilkoti). Briefly, eligible patients included in
619 the repository were men and women ages 18 years and above that were admitted to an adult ICU at Duke
620 University Hospital with SARS-CoV-2 infection confirmed by PCR testing. Samples were collected on study days
621 1, 3, 7, 14, and 21. In addition to biological samples, clinical data on these patients were also collected including
622 demographics, laboratory data, and clinical course. All data reported in this paper were obtained with patient
623 samples from the Duke ICU Biorepository and this study was performed in collaboration with Biorepository team.

624 Negative control plasma samples were collected under a normal blood donor protocol (Pro00009459, PI
625 Tony Moody) and range in collection dates from 2014 to 2019 (prior to the COVID-19 outbreak). All patient
626 information, including demographics, is unknown to the investigator team. These samples were accessed via an
627 exempted protocol approved by the Duke University Institutional review board (Pro00105331, PI Ashutosh
628 Chilkoti).

629 Blood was either purchased commercially (Innovative Research, Inc.) or accessed from the ICU
630 biorepository (Pro00101196, PI Bryan Kraft) in EDTA-collection tubes and was tested within 48 hours of sample
631 collection.

632 Live SARS-CoV-2 Microneutralization assay (MN)

633 The SARS-CoV-2 virus (Isolate USA-WA1/2020, NR-52281) was deposited by the Centers for Disease
634 Control and Prevention and obtained through BEI Resources, NIAID, NIH. SARS-CoV-2 Micro-neutralization
635 (MN) assays were adapted from a previous study⁵¹. In short, plasma samples are diluted two-fold and incubated
636 with 100 TCID50 virus for 1 h. These dilutions are transferred to a 96 well plate containing 2×10^4 Vero E6 cells
637 per well. Following a 96 h incubation, cells were fixed with 10% formalin and CPE was determined after staining
638 with 0.1% crystal violet. Each batch of MN includes a known neutralizing control antibody (Clone D001; SINO,
639 CAT# 40150-D001). Data are reported as the inverse of the last dilution of plasma that protected from CPE,
640 \log_{10} transformed.

641 IP-10 experiments

642 Open format DA-D4 slides were fabricated as described above using all reagents needed for antibody
643 detection and IP-10 detection. Citrated plasma samples from 10 patients were procured from the ICU

644 biorepository. 60 μ L of each sample was added to two separate DA-D4 chips, incubated for 30 min, and the
645 chips were then rinsed using 0.1% Tween in 1x PBS. All slides were scanned with the Genepix tabletop scanner.

646 IP-10 levels were measured using the LEGENDplex™ Human Proinflammatory Chemokine Panel (13-
647 plex) and LEGENDplex™ Human Anti-Virus Response Panel (13-plex) obtained from BioLegend. Assays were
648 performed with patient serum per the manufacturer's instructions. The assay was performed using a Beckman
649 Coulter CytoFLEX flow cytometer and data processing was performed using BioLegend's Bio-Bits cloud-based
650 software platform. Each sample was tested in triplicate, and the results are reported as mean of these triplicates.

651 Statistical analysis

652 Statistical analysis was performed using GraphPad Prism version 8.4.1 (GraphPad Software, Inc). All
653 data were log transformed for analysis. To establish statistical significance between two groups (Fig. 2a-c),
654 unpaired t-tests were used. When comparing multiple groups, a one-way ANOVA followed by Tukey's post-hoc
655 multiple comparisons test was used. Pearson r correlation was used to assess the degree of correlation between
656 measurements.

657 **Acknowledgments**

658 AC acknowledges the support of the National Science Foundation (Grant No. CBET202936); the National
659 Cancer Institute through grants P30-CA014236, R01-CA248491, UH3-CA211232; Department of Defense
660 United States Special Operations Command (Grant No. W81XWH-16-C-0219); Defence Academy of the United
661 Kingdom (Grant No. ACC6010469); and the Combat Casualty Care Research Program (JPC-6) (Grant No.
662 W81XWH-17-2-0045). BDK receives funding from NHLBI (K08HL130557). We thank Dr. David Montefiori for
663 providing laboratory space to complete the clinical validation studies. We also thank Rebecca Sahm for
664 completing live SARS-CoV-2 microneutralization assays, which were performed in the Virology Unit of the Duke
665 Regional Biocontainment Laboratory, which received partial support for construction from the NIH/NIAD
666 (UC6AI058607; GDS). We thank the nurses in the intensive care units of Duke University Hospital for collecting
667 the blood samples used for this study and thank Dr. Patty Lee for supporting the ICU Biorepository. We thank
668 Dr. Tony Moody for access to the pre-pandemic negative control samples used in this study, Dr. Thomas Denny
669 for providing access to BSL2+ laboratory facilities to run the pre-pandemic negative samples, and Heidi Register
670 for assistance with testing the negative samples on the DA-D4 POCT.

671 **Author Contribution**

672 JTH and DSK are co-lead authors, who equally participated in experimental design, data collection, data
673 analysis, manuscript drafting, figure creation and manuscript revision. LBO participated in experimental design,
674 and collection and analysis of data for clinical validation. JL developed the D4Scope used throughout the study
675 and drafted text and figures related to the D4Scope. DSK, CMF, and AMH developed the microfluidic cassette.
676 GK cloned, expressed, and purified the N-NTD. SAW participated in data collection and analysis. CMF, DYJ,
677 and AMH were responsible for conceptualization, investigation, and manuscript revision. CFP oversaw statistical
678 analysis and assisted in study design. TO designed and ran live virus microneutralization assays, analyzed data
679 and participated in writing the manuscript. GDS participated in writing the manuscript. BDK, CWW, LC, LGQ,
680 SKN, BAS, IAN, and LBO contributed to the development of the Duke COVID-19 biorepositories and oversaw
681 clinical data acquisition. BDK and CWW participated in manuscript revision. AC is the principal investigator who
682 directed the studies, helped plan experiments, analyzed data, and participated in writing and editing the
683 manuscript. All authors read and approved the manuscript.

684 **Ethics declarations**

685 Immucor Inc., has acquired the rights to the D4 assay on POEGMA brushes for in vitro diagnostics from
686 Sentilus Inc. (cofounded by AC and AMH).

689

References

- 690 1 Dong, E., Du, H. & Gardner, L. An interactive web-based dashboard to track COVID-19 in real time. *Lancet Infect Dis* **20**, 533-534, doi:10.1016/S1473-3099(20)30120-1 (2020).
- 691 2 Huang, C. *et al.* Clinical features of patients infected with 2019 novel coronavirus in Wuhan, China. *Lancet* **395**, 497-506, doi:10.1016/S0140-6736(20)30183-5 (2020).
- 692 3 Rothe, C. *et al.* Transmission of 2019-nCoV Infection from an Asymptomatic Contact in Germany. *N Engl J Med* **382**, 970-971, doi:10.1056/NEJMc2001468 (2020).
- 693 4 Wiersinga, W. J., Rhodes, A., Cheng, A. C., Peacock, S. J. & Prescott, H. C. Pathophysiology, Transmission, Diagnosis, and Treatment of Coronavirus Disease 2019 (COVID-19): A Review. *JAMA*, doi:10.1001/jama.2020.12839 (2020).
- 694 5 Miller, I. F., Becker, A. D., Grenfell, B. T. & Metcalf, C. J. E. Disease and healthcare burden of COVID-19 in the United States. *Nat Med* **26**, 1212-1217, doi:10.1038/s41591-020-0952-y (2020).
- 695 6 Liu, Q. *et al.* The experiences of health-care providers during the COVID-19 crisis in China: a qualitative study. *Lancet Glob Health* **8**, e790-e798, doi:10.1016/S2214-109X(20)30204-7 (2020).
- 696 7 Tang, Y. W., Schmitz, J. E., Persing, D. H. & Stratton, C. W. Laboratory Diagnosis of COVID-19: Current Issues and Challenges. *J Clin Microbiol* **58**, doi:10.1128/JCM.00512-20 (2020).
- 697 8 Chu, D. K. W. *et al.* Molecular Diagnosis of a Novel Coronavirus (2019-nCoV) Causing an Outbreak of Pneumonia. *Clin Chem* **66**, 549-555, doi:10.1093/clinchem/hvaa029 (2020).
- 698 9 Lieberman, J. A. *et al.* Comparison of Commercially Available and Laboratory-Developed Assays for In Vitro Detection of SARS-CoV-2 in Clinical Laboratories. *J Clin Microbiol* **58**, doi:10.1128/JCM.00821-20 (2020).
- 699 10 Nalla, A. K. *et al.* Comparative Performance of SARS-CoV-2 Detection Assays Using Seven Different Primer-Probe Sets and One Assay Kit. *J Clin Microbiol* **58**, doi:10.1128/JCM.00557-20 (2020).
- 700 11 Wölfel, R. *et al.* Virological assessment of hospitalized patients with COVID-2019. *Nature* **581**, 465-469, doi:10.1038/s41586-020-2196-x (2020).
- 701 12 Krammer, F. & Simon, V. Serology assays to manage COVID-19. *Science* **368**, 1060-1061, doi:10.1126/science.abc1227 (2020).
- 702 13 Bryant, J. E. *et al.* Serology for SARS-CoV-2: Apprehensions, opportunities, and the path forward. *Sci Immunol* **5**, doi:10.1126/sciimmunol.abc6347 (2020).
- 703 14 Atyeo, C. *et al.* Distinct Early Serological Signatures Track with SARS-CoV-2 Survival. *Immunity*, doi:10.1016/j.immuni.2020.07.020 (2020).
- 704 15 Long, Q. X. *et al.* Antibody responses to SARS-CoV-2 in patients with COVID-19. *Nat Med* **26**, 845-848, doi:10.1038/s41591-020-0897-1 (2020).
- 705 16 Yong, S. E. F. *et al.* Connecting clusters of COVID-19: an epidemiological and serological investigation. *Lancet Infect Dis* **20**, 809-815, doi:10.1016/S1473-3099(20)30273-5 (2020).
- 706 17 Lipsitch, M., Kahn, R. & Mina, M. J. Antibody testing will enhance the power and accuracy of COVID-19-prevention trials. *Nat Med* **26**, 818-819, doi:10.1038/s41591-020-0887-3 (2020).
- 707 18 Khailany, R. A., Safdar, M. & Ozaslan, M. Genomic characterization of a novel SARS-CoV-2. *Gene Rep*, 100682, doi:10.1016/j.genrep.2020.100682 (2020).
- 708 19 Lisboa Bastos, M. *et al.* Diagnostic accuracy of serological tests for covid-19: systematic review and meta-analysis. *BMJ* **370**, m2516, doi:10.1136/bmj.m2516 (2020).
- 709 20 Whitman, J. D. *et al.* Evaluation of SARS-CoV-2 serology assays reveals a range of test performance. *Nat Biotechnol*, doi:10.1038/s41587-020-0659-0 (2020).
- 710 21 Amanat, F. *et al.* A serological assay to detect SARS-CoV-2 seroconversion in humans. *Nat Med* **26**, 1033-1036, doi:10.1038/s41591-020-0913-5 (2020).
- 711 22 Okba, N. M. A. *et al.* Severe Acute Respiratory Syndrome Coronavirus 2-Specific Antibody Responses in Coronavirus Disease Patients. *Emerg Infect Dis* **26**, 1478-1488, doi:10.3201/eid2607.200841 (2020).
- 712 23 Rogers, T. F. *et al.* Isolation of potent SARS-CoV-2 neutralizing antibodies and protection from disease in a small animal model. *Science* **369**, 956-963, doi:10.1126/science.abc7520 (2020).
- 713 24 Crowther, J. R. The ELISA guidebook. *Methods Mol Biol* **149**, III-IV, 1-413, doi:10.1385/1592590497 (2000).
- 714 25 Posthuma-Trumpie, G. A., Korf, J. & van Amerongen, A. Lateral flow (immuno)assay: its strengths, weaknesses, opportunities and threats. A literature survey. *Anal Bioanal Chem* **393**, 569-582, doi:10.1007/s00216-008-2287-2 (2009).

742

- 743 26 Ponti, G., Maccaferri, M., Ruini, C., Tomasi, A. & Ozben, T. Biomarkers associated with COVID-19
744 disease progression. *Crit Rev Clin Lab Sci* **57**, 389-399, doi:10.1080/10408363.2020.1770685 (2020).
- 745 27 Laing, A. G. *et al.* A dynamic COVID-19 immune signature includes associations with poor prognosis.
746 *Nat Med*, doi:10.1038/s41591-020-1038-6 (2020).
- 747 28 Joh, D. Y. *et al.* Inkjet-printed point-of-care immunoassay on a nanoscale polymer brush enables
748 subpicomolar detection of analytes in blood. *Proc Natl Acad Sci U S A* **114**, E7054-E7062,
749 doi:10.1073/pnas.1703200114 (2017).
- 750 29 Ravichandran, S. *et al.* Antibody signature induced by SARS-CoV-2 spike protein immunogens in
751 rabbits. *Sci Transl Med* **12**, doi:10.1126/scitranslmed.abc3539 (2020).
- 752 30 Ahmed, S. F., Quadeer, A. A. & McKay, M. R. Preliminary Identification of Potential Vaccine Targets for
753 the COVID-19 Coronavirus (SARS-CoV-2) Based on SARS-CoV Immunological Studies. *Viruses* **12**,
754 doi:10.3390/v12030254 (2020).
- 755 31 Dutta, N. K., Mazumdar, K. & Gordy, J. T. The Nucleocapsid Protein of SARS-CoV-2: a Target for
756 Vaccine Development. *J Virol* **94**, doi:10.1128/JVI.00647-20 (2020).
- 757 32 Cong, Y. *et al.* Nucleocapsid Protein Recruitment to Replication-Transcription Complexes Plays a
758 Crucial Role in Coronaviral Life Cycle. *J Virol* **94**, doi:10.1128/JVI.01925-19 (2020).
- 759 33 Jiang, S., Hillyer, C. & Du, L. Neutralizing Antibodies against SARS-CoV-2 and Other Human
760 Coronaviruses: (Trends in Immunology 41, 355-359; 2020). *Trends Immunol* **41**, 545,
761 doi:10.1016/j.it.2020.04.008 (2020).
- 762 34 Lu, R. *et al.* Genomic characterisation and epidemiology of 2019 novel coronavirus: implications for
763 virus origins and receptor binding. *Lancet* **395**, 565-574, doi:10.1016/S0140-6736(20)30251-8 (2020).
- 764 35 Kang, S. *et al.* Crystal structure of SARS-CoV-2 nucleocapsid protein RNA binding domain reveals
765 potential unique drug targeting sites. *Acta Pharm Sin B*, doi:10.1016/j.apsb.2020.04.009 (2020).
- 766 36 Rosadas, C., Randell, P., Khan, M., McClure, M. O. & Tedder, R. S. Testing for responses to the wrong
767 SARS-CoV-2 antigen? *Lancet* **396**, e23, doi:10.1016/S0140-6736(20)31830-4 (2020).
- 768 37 Liu, L. *et al.* High neutralizing antibody titer in intensive care unit patients with COVID-19. *Emerg*
769 *Microbes Infect* **9**, 1664-1670, doi:10.1080/22221751.2020.1791738 (2020).
- 770 38 Zhao, J. *et al.* Antibody responses to SARS-CoV-2 in patients of novel coronavirus disease 2019. *Clin*
771 *Infect Dis*, doi:10.1093/cid/ciaa344 (2020).
- 772 39 McAndrews, K. M. *et al.* Heterogeneous antibodies against SARS-CoV-2 spike receptor binding domain
773 and nucleocapsid with implications for COVID-19 immunity. *JCI Insight* **5**,
774 doi:10.1172/jci.insight.142386 (2020).
- 775 40 Vaninov, N. In the eye of the COVID-19 cytokine storm. *Nat Rev Immunol* **20**, 277, doi:10.1038/s41577-
776 020-0305-6 (2020).
- 777 41 Yang, Y. *et al.* Plasma IP-10 and MCP-3 levels are highly associated with disease severity and predict
778 the progression of COVID-19. *J Allergy Clin Immunol* **146**, 119-127 e114,
779 doi:10.1016/j.jaci.2020.04.027 (2020).
- 780 42 Armbruster, D. A. & Pry, T. Limit of blank, limit of detection and limit of quantitation. *Clin Biochem Rev*
781 **29 Suppl 1**, S49-52 (2008).
- 782 43 McElvaney, O. J. *et al.* A linear prognostic score based on the ratio of interleukin-6 to interleukin-10
783 predicts outcomes in COVID-19. *EBioMedicine* **61**, 103026, doi:10.1016/j.ebiom.2020.103026 (2020).
- 784 44 Winter, A. K. & Hegde, S. T. The important role of serology for COVID-19 control. *Lancet Infect Dis* **20**,
785 758-759, doi:10.1016/S1473-3099(20)30322-4 (2020).
- 786 45 Waterboer, T., Sehr, P. & Pawlita, M. Suppression of non-specific binding in serological Luminex
787 assays. *J Immunol Methods* **309**, 200-204, doi:10.1016/j.jim.2005.11.008 (2006).
- 788 46 Heggstad, J. T., Fontes, C. M., Joh, D. Y., Hucknall, A. M. & Chilkoti, A. In Pursuit of Zero 2.0: Recent
789 Developments in Nonfouling Polymer Brushes for Immunoassays. *Adv Mater* **32**, e1903285,
790 doi:10.1002/adma.201903285 (2020).
- 791 47 Hucknall, A. *et al.* Simple Fabrication of Antibody Microarrays on Nonfouling Polymer Brushes with
792 Femtomolar Sensitivity for Protein Analytes in Serum and Blood. *Adv Mater* **21**, 1968-1971,
793 doi:10.1002/adma.200803125 (2009).
- 794 48 Hucknall, A., Rangarajan, S. & Chilkoti, A. In Pursuit of Zero: Polymer Brushes that Resist the
795 Adsorption of Proteins. *Advanced Materials* **21**, 2441-2446, doi:10.1002/adma.200900383 (2009).

- 796 49 Norman, M. *et al.* Ultrasensitive high-resolution profiling of early seroconversion in patients with
797 COVID-19. *Nat Biomed Eng*, doi:10.1038/s41551-020-00611-x (2020).
- 798 50 Seow, J. *et al.* Longitudinal evaluation and decline of antibody responses in SARS-CoV-2 infection.
799 *medRxiv*, 2020.2007.2009.20148429, doi:10.1101/2020.07.09.20148429 (2020).
- 800 51 Berry, J. D. *et al.* Development and characterisation of neutralising monoclonal antibody to the SARS-
801 coronavirus. *J Virol Methods* **120**, 87-96, doi:10.1016/j.jviromet.2004.04.009 (2004).
802
803
804